

Supplementary Materials

Fig. S1. Induction of type I IFN in cDCs by Heat-iMVA requires cGAS, STING, IRF3, IRF7 and IFNAR1.

Fig. S2. Induction of type I IFN in cDCs by UV-iMVA requires also requires STING.

Fig. S3. Induction of PD-L1 expression on Heat-iMVA-infected B16-F10 cells.

Fig. S4. Induction of type I IFN, proinflammatory cytokines and chemokines, and PD-L1 expression in human melanoma cell line infected with Heat-iMVA.

Fig. S5. Intratumoral injection of Heat-iMVA results in the generation of Granzyme B⁺ and Ki67⁺ CD8⁺ and CD4⁺ T cells in the TNDLs.

Fig. S6. Initial B16-F10 tumor volumes at the time of the first injection.

Fig. S7. Intratumoral injection of Heat-iMVA leads to the generation of anti-tumor specific CD8⁺ T cells in the TDLNs in a Batf3-dependent manner.

Fig. S8. Intraperitoneal delivery of anti-CTLA-4, anti-PD1, or anti-PD-L1 antibody has minimum survival benefit in a unilateral B16-F10 melanoma implantation model.

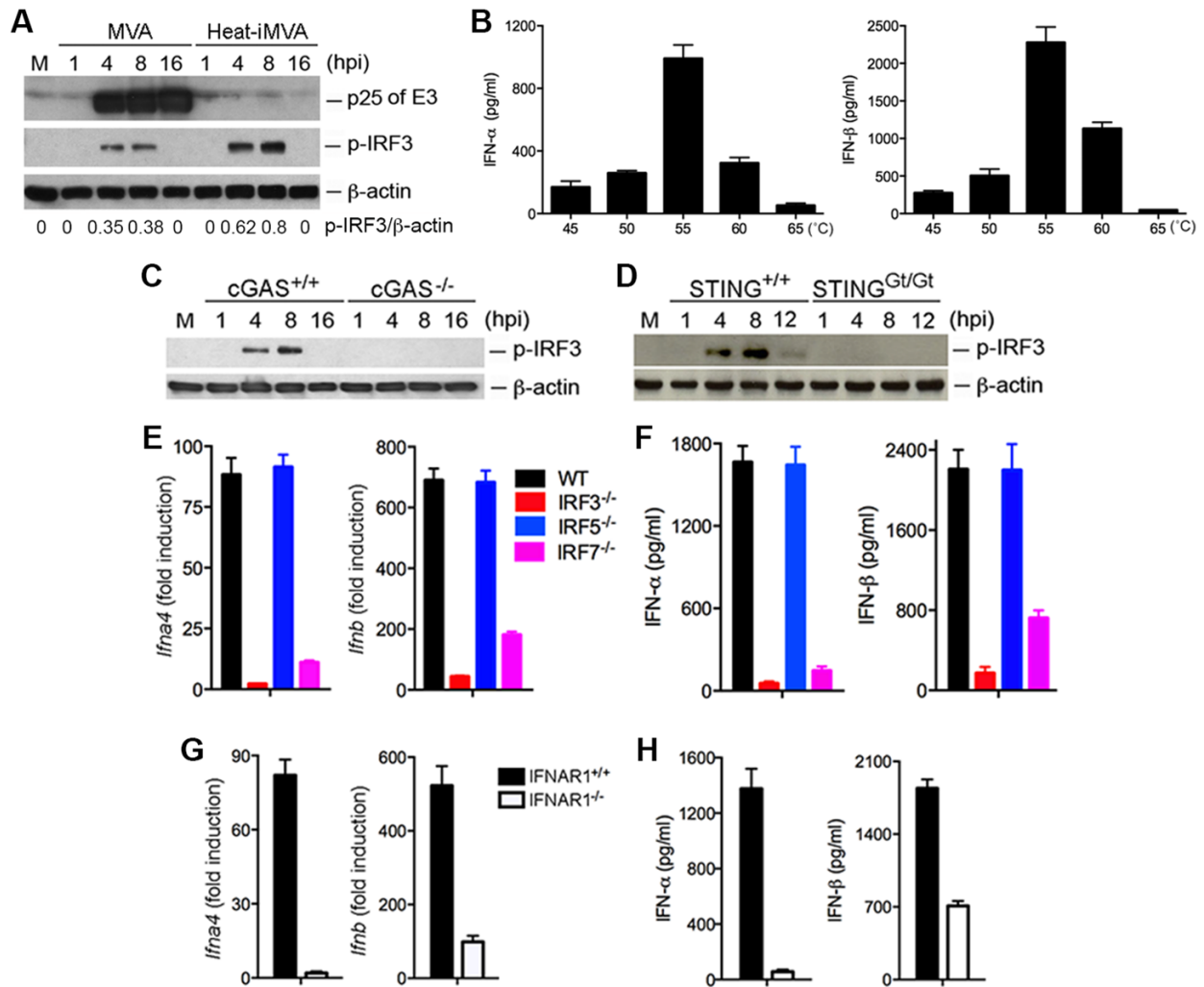
Fig. S9. The combination of intratumoral injection of Heat-MVA with systemic delivery of anti-CTLA-4 or anti-PD-L1 antibodies significantly increases the overall response and cure rates in a MC38 bilateral tumor implantation model.

Fig. S10. Intratumoral injection of Heat-iMVA is more effective than poly (I:C) in treating large established tumors.

Fig. S11. The combination of intratumoral injection of Heat-MVA with systemic delivery of immune checkpoint antibodies has synergistic effect in curing large established B16-F10 melanomas.

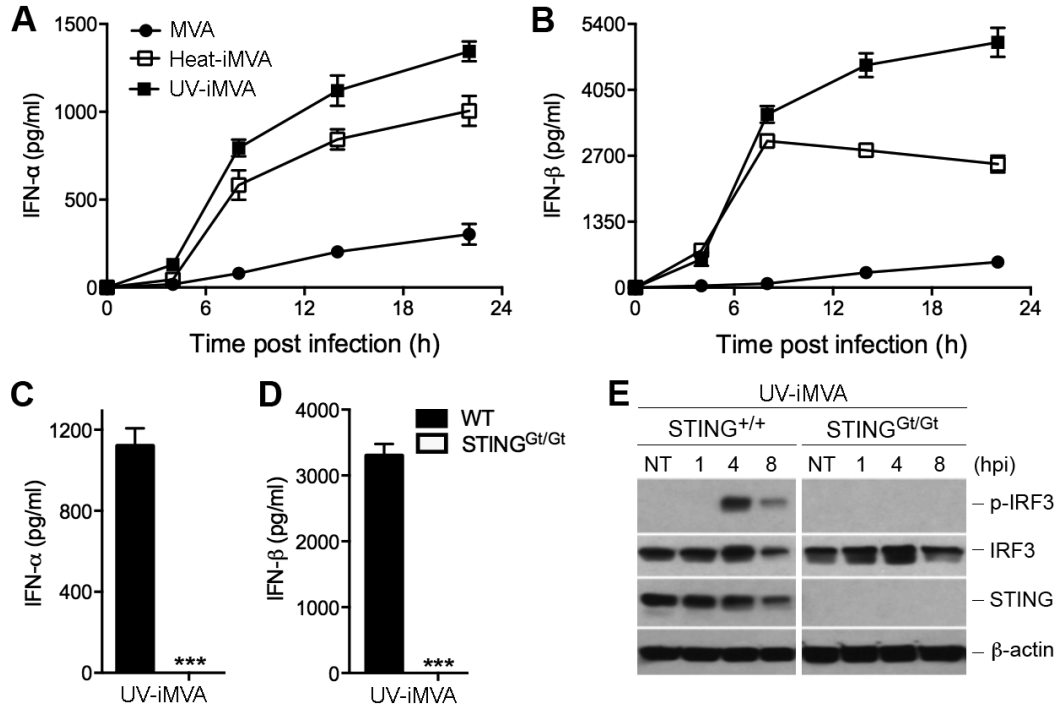
Table S1. Primer sequences for quantitative real-time PCR for the expression of type I IFN, proinflammatory cytokine and chemokine genes.

Supplementary Materials

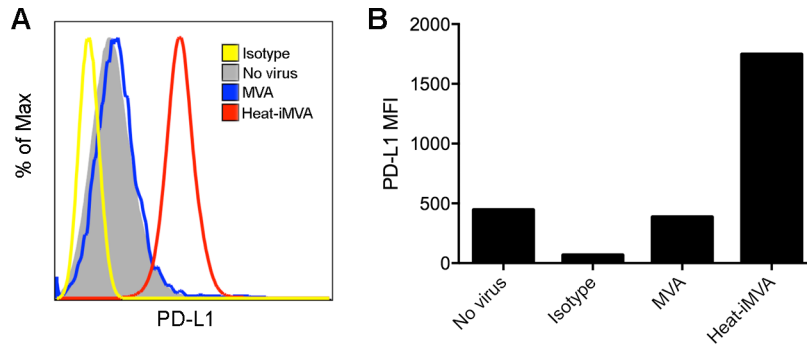


1 Fig. S1. Induction of type I IFN in murine cDCs by Heat-iMVA requires cGAS, STING,
 2 IRF3, IRF7 and IFNAR1. (A) Western blot showing protein levels of p-IRF3 and vaccinia E3
 3 in Heat-iMVA or MVA-infected cDCs. The ratios of p-IRF3/β-actin were shown. (B) The effect
 4 of heating temperature on the abilities of heat-iMVA to induce IFN-α and IFN-β secretion in
 5 infected cDCs. (C, D) Heat-iMVA infection of cDCs induces phosphorylation of IRF3 that is
 6 dependent on cGAS (C) and STING (D). Western blot showing protein levels of p-IRF3 and β-
 7 actin in Heat-iMVA-infected cDCs from cGAS^{+/+} and cGAS^{-/-} mice (C) and from STING^{+/+} and
 8 STING^{Gt/Gt} mice (D). “hpi”, hours post infection. “M”, mock infection control. (E) *Ifna4* and *Ifnb*
 9 relative mRNA expression compared with no virus control in cDCs generated from WT, IRF3^{-/-},
 10 IRF7^{-/-}, or IRF5^{-/-} mice and infected with Heat-iMVA. Data are means ± SEM (n=3). (F)

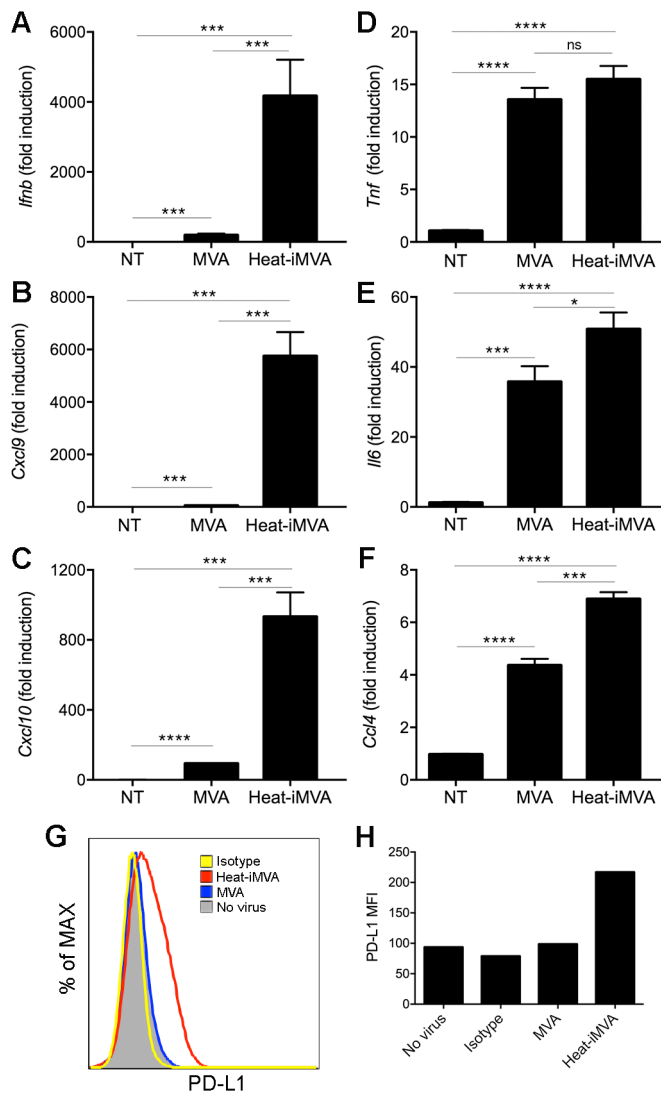
11 Concentrations of secreted IFN- α and IFN- β in the medium of cDCs generated from WT, IRF3^{-/-},
12 IRF7^{-/-}, or IRF5^{-/-} mice and infected with Heat-iMVA. Data are means \pm SEM (n=3). (G) *Ifna4*
13 and *Ifnb* relative mRNA expression compared with no virus control in cDCs generated from
14 IFNAR1^{+/+} and IFNAR1^{-/-} mice and infected with Heat-iMVA. Data are means \pm SEM (n=3).
15 (F) Concentrations of secreted IFN- α and IFN- β in the medium of cDCs generated from
16 IFNAR1^{+/+} and IFNAR1^{-/-} mice and infected with Heat-iMVA. Data are means \pm SEM (n=3).



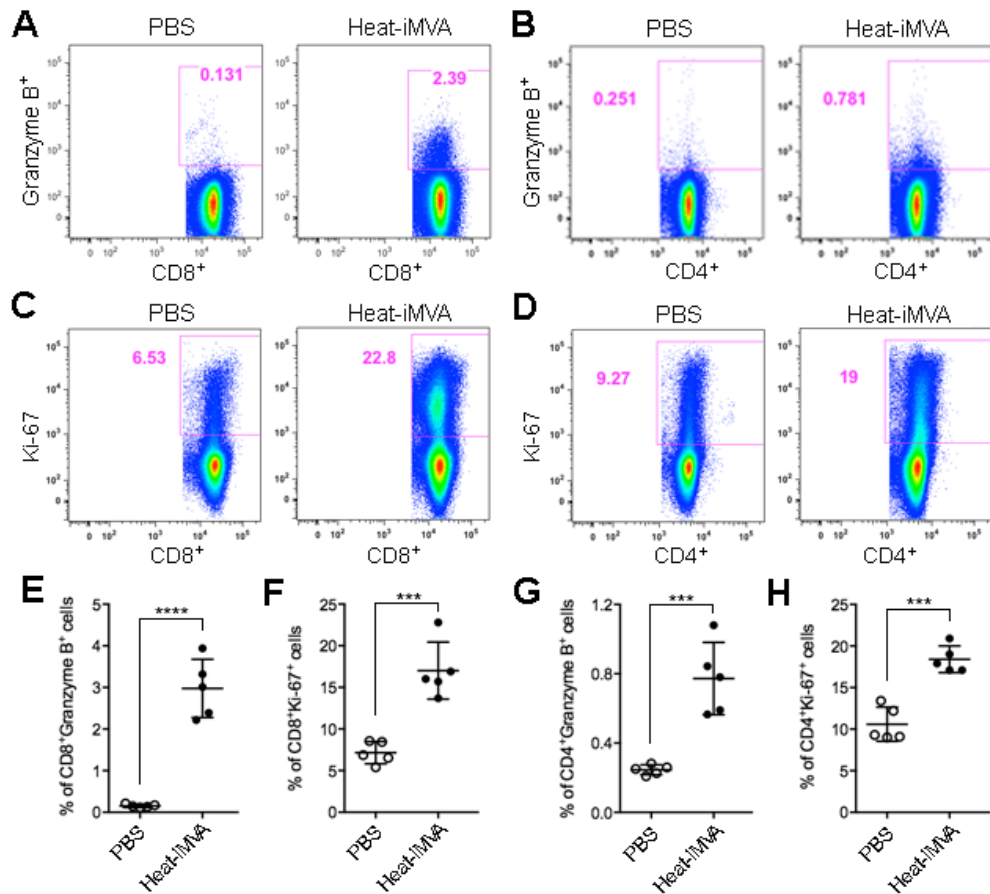
30 Fig. S2. Induction of type I IFN in cDCs by UV-iMVA requires also requires STING. (A, B)
 31 The concentrations of secreted IFN- α (A) and IFN- β (B) in the medium over time following
 32 MVA, Heat-iMVA, or UV-iMVA infection of cDCs. Data are means \pm SEM (n=3). (C, D)
 33 Concentrations of secreted IFN- α (C) and IFN- β (D) in the medium of cDCs generated from WT
 34 and STING^{Gt/Gt} mice and infected with UV-iMVA. (n=3; *** P < 0.001; t test). (E) Western Blot
 35 showing protein levels of p-IRF-3, IRF3, STING, and β -actin. "hpi", hours post infection. "NT",
 36 no treatment control.



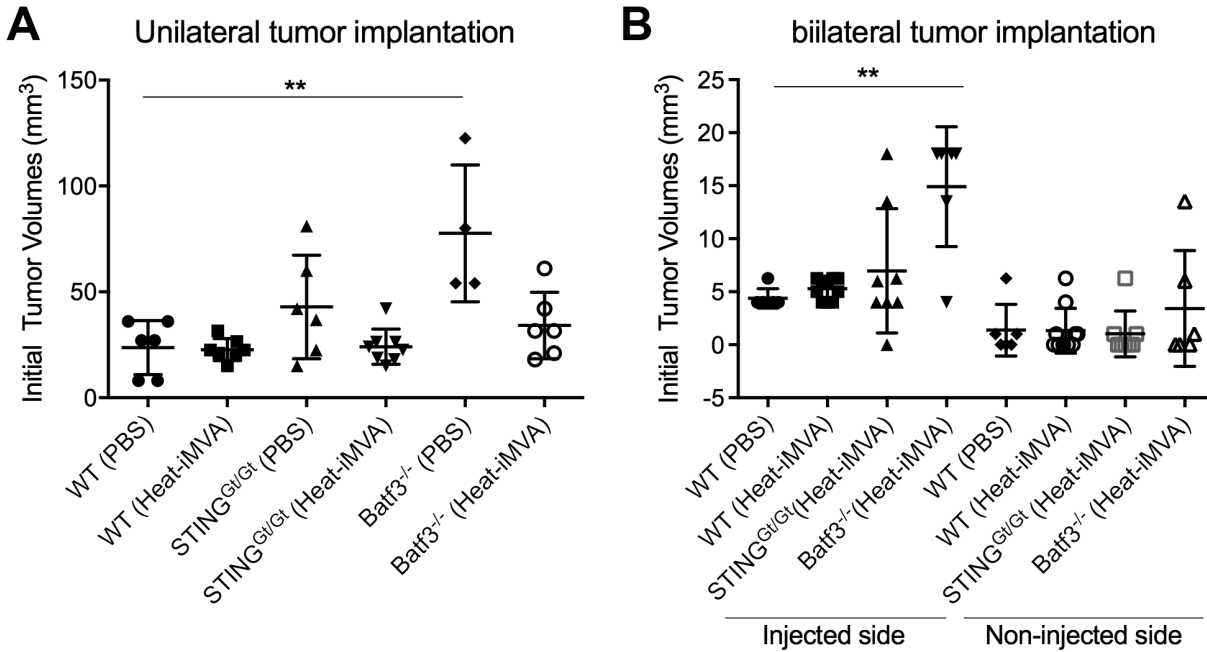
37 Fig. S3. **Induction of PD-L1 expression on Heat-iMVA-infected B16-F10 cells.** (A)
 38 Representative flow cytometry plot of B16-F10 cells infected with either MVA at a MOI of 10 or
 39 with an equivalent amount of Heat-iMVA. No virus infection and isotype control were also
 40 included. (B) The mean fluorescence intensity (MFI) of PD-L1 expression on B16-F10 cells
 41 infected with either MVA, Heat-iMVA, or mock infection control is shown.



42 Fig. S4. Induction of type I IFN, proinflammatory cytokines and chemokines, and PD-L1
 43 expression in human melanoma cell line infected with Heat-iMVA. (A-F) Human melanoma
 44 cell line SK-MEL-146 cells were infected with MVA at a MOI of 10 or with an equivalent
 45 amount of Heat-iMVA. Cells were collected at 6 h post infection and RNAs were extracted.
 46 Quantitative real-time PCR was performed. The relative mRNA expression of *Ifnb*, *Cxcl9*,
 47 *Cxcl10*, *Tnf*, *Il6*, *Ccl4*, and *Ccl5* in B16-F10 cells infected with either MVA or Heat-iMVA.
 48 (n=3; *** $P < 0.001$; **** $P < 0.0001$; t test). (G, H) Expression of PD-L1 on SK-MEL-146 cells
 49 infected with either MVA, Heat-iMVA or mock infection control. Representative flow cytometry
 50 plot is shown in (G), repeated once. (H) The mean fluorescence intensity (MFI) of PD-L1
 51 expression on SK-MEL-146 cells infected with either MVA, Heat-iMVA, or mock infection
 52 control is shown.



53 Fig. S5. **Intratumoral injection of Heat-iMVA results in the generation of Granzyme B⁺ and**
 54 **Ki67⁺ CD8⁺ and CD4⁺ T cells in the TNDLs.** 5 x 10⁵ B16-F10 melanoma cells were implanted
 55 intradermally to the right flank of the mice. Seven days post implantation, either Heat-iMVA (an
 56 equivalent of 2x 10⁷ pfu of MVA) or PBS were injected into the tumors on the right flank. The
 57 injections were repeated three days later. TDLNs were harvested 3 days post last injection and
 58 cell suspensions were generated. Immune cells were stained with various markers and analyzed
 59 by FACS. (A-D) Representative flow cytometry plot of CD8⁺ cells expressing Granzyme B⁺ (A)
 60 or Ki-67 (C), CD4⁺ cells expressing Granzyme B (B), or Ki-67 (D). (E-H) Percentages of
 61 CD8⁺Granzyme B⁺ (E), CD8⁺Ki-67⁺ (F), CD4⁺Granzyme B⁺ (G), and CD4⁺Ki67⁺ (H) cells
 62 within TNLNs of mice treated with PBS (n=5) or Heat-iMVA (n=5; ****P* < 0.001; *****P* <
 63 0.0001; *t* test). A representative experiment is shown, repeated once.



64 Fig. S6. **Initial B16-F10 tumor volumes at the time of the first injection.** (A) Unilateral tumor
 65 implantation model. B16-F10 melanoma cells (1×10^5 cells) were intradermally implanted into
 66 the right flank of WT C57B/6, STING^{Gt/Gt}, or Batf3^{-/-} mice. At 11 days post-implantation, the
 67 tumors were injected with either Heat-iMVA (equivalent of 2×10^7 pfu) or PBS twice weekly.
 68 The initial tumor volumes at the time of first injection are shown ($n=5$; $**P < 0.01$; t test). (B)
 69 Bilateral tumor implantation model. B16-F10 melanoma cells were implanted intradermally to
 70 the left and right flanks of C57B/6 mice (5×10^5 to the right flank and 1×10^5 to the left flank). 8
 71 days after tumor implantation, Heat-iMVA or PBS was injected to the larger tumors on the right
 72 flank. The initial tumor volumes at the time of first injection are shown ($n=5, 6$; $**P < 0.01$; t
 73 test).

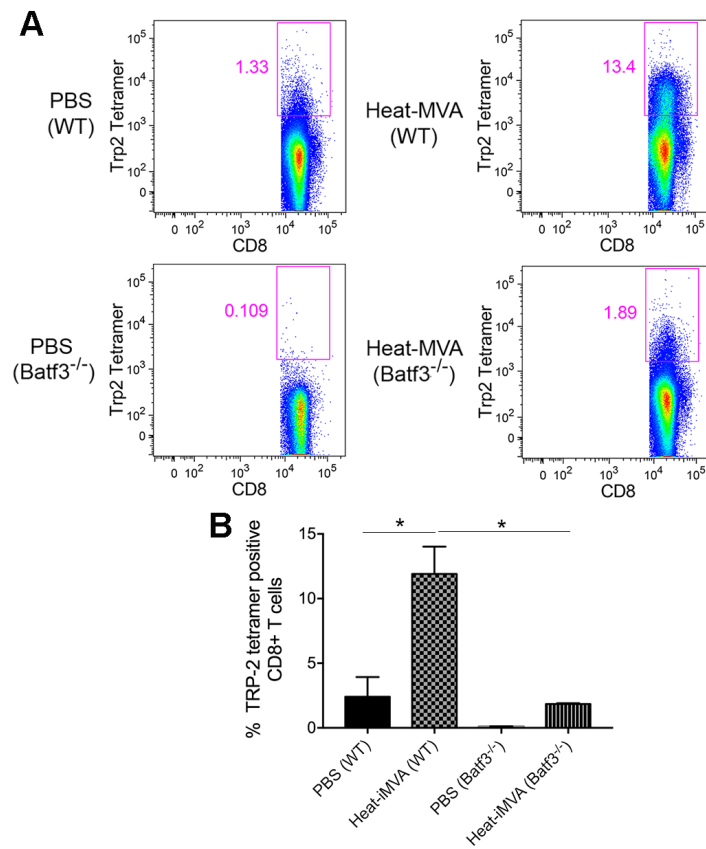
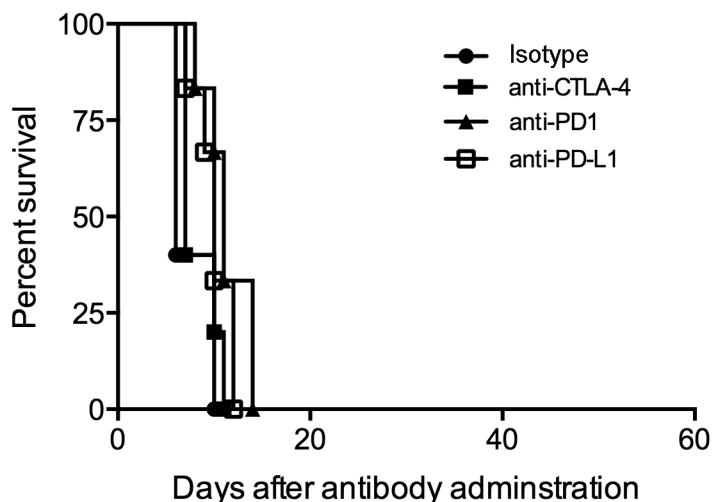
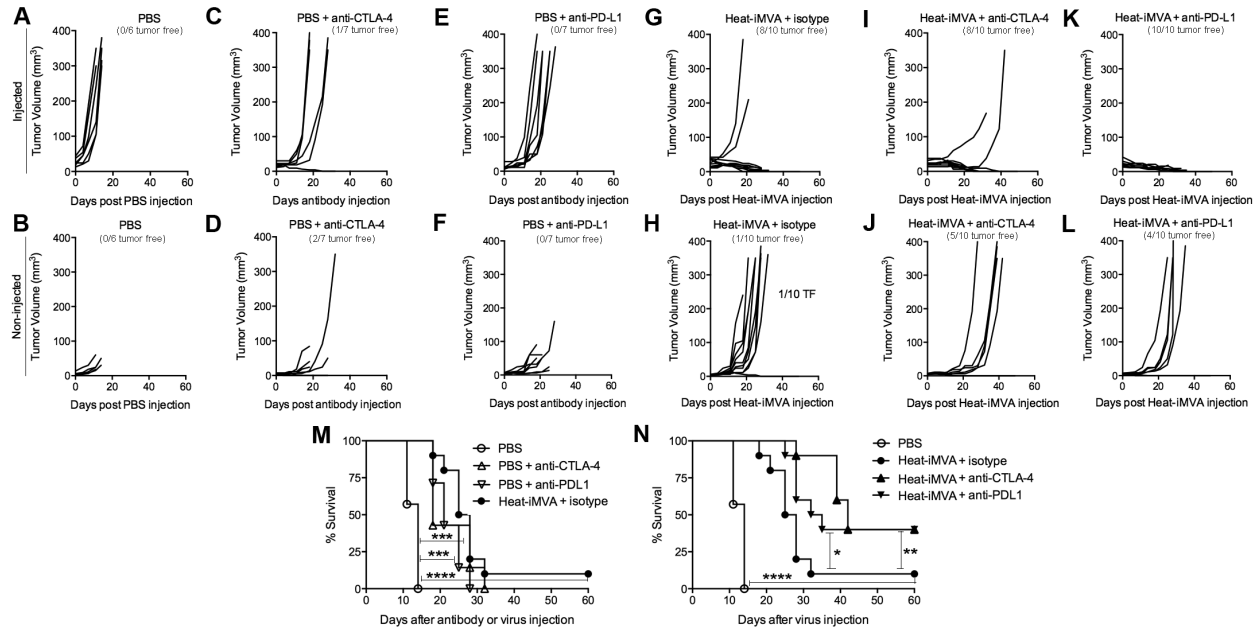


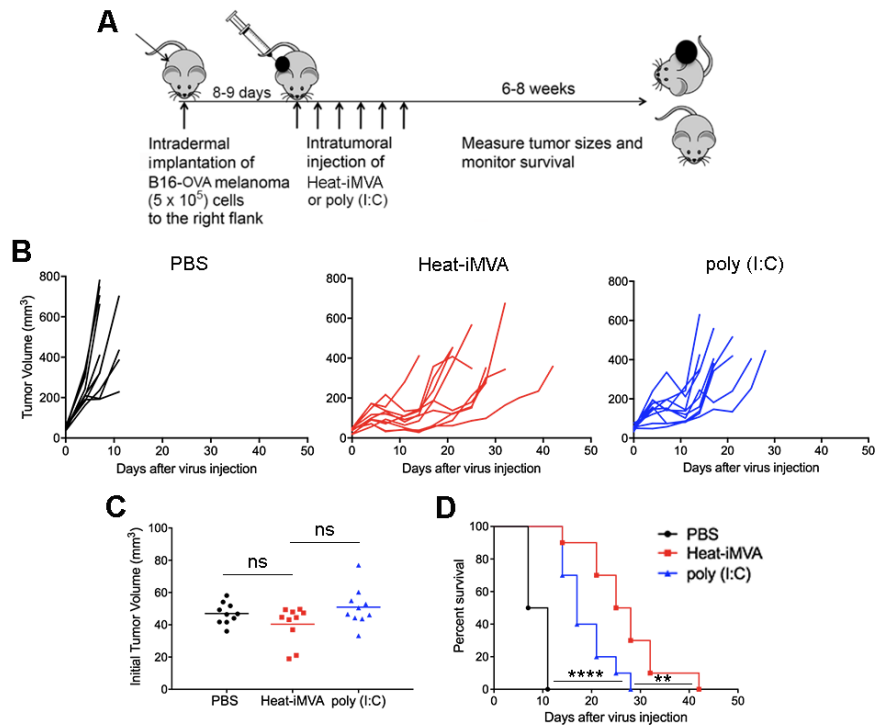
Fig. S7. Intratumoral injection of Heat-iMVA leads to the generation of anti-tumor specific CD8⁺ T cells in the TDLNs in a Batf3-dependent manner. (A) Representative flow cytometry plots of TRP-2 tetramer positive CD8⁺ T cells in TDLNs in a B16-F10 melanoma model treated with either PBS or Heat-inactivated MVA. (B) Percentages of TRP-2 tetramer positive CD8⁺ T cells in WT and Batf3^{-/-} mice with B16-F10 melanomas treated with either PBS or Heat-MVA. Each sample was from lymph nodes pooled from 2-3 mice treated with the same condition (n=3; *P < 0.05; *t* test).



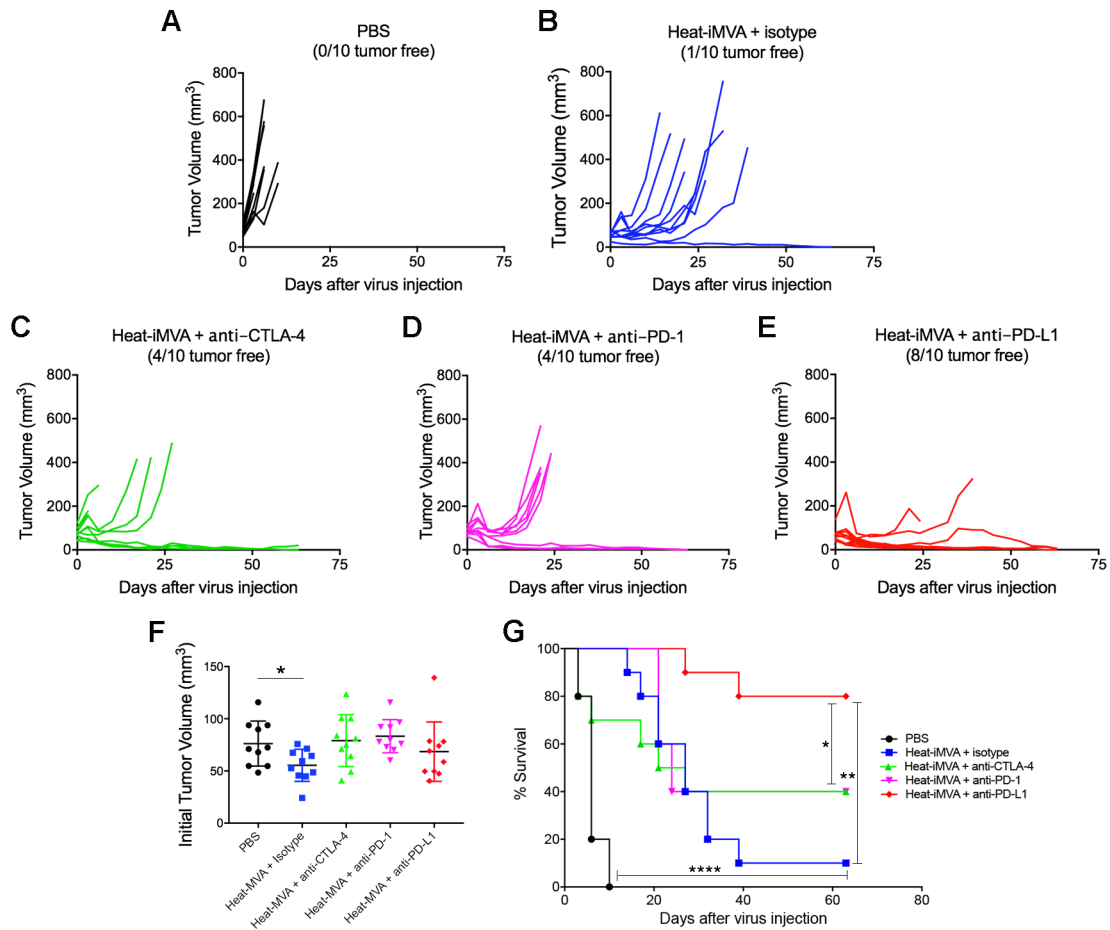
74 Fig. S8. **Intraperitoneal delivery of anti-CTLA-4, anti-PD1, or anti-PD-L1 antibody has**
 75 **minimum survival benefit in a unilateral B16-F10 melanoma implantation model.** B16-F10
 76 melanoma (1×10^5 cells) were implanted intradermally into the shaved skin on the right flank of
 77 WT C57BL/6J mice. 8 days post implantation, mice were treated with intraperitoneal delivery of
 78 anti-CTLA-4 (100 μ g), anti-PD1 (250 μ g), anti-PD-L1 (250 μ g), or isotype control twice a week
 79 (every 3-4 days). Kaplan-Meier survival curve is shown for isotype control (n=5), anti-CTLA-4-
 80 treated mice (n=6), anti-PD1-treated mice (n=6), and anti-PD-L1-treated mice (n=6).



81
 82 **Fig. S9. The combination of intratumoral injection of Heat-MVA with systemic delivery of**
 83 **anti-CTLA-4 or anti-PD-L1 antibodies significantly increases the overall response and cure**
 84 **rates in a MC38 bilateral tumor implantation model. (A-L) Volumes of injected (A) and non-**
 85 **injected (B) tumor volume over days after PBS injection, after intratumoral injection of PBS and**
 86 **intraperitoneal delivery of anti-CTLA-4 antibody (C, D), after intratumoral injection of PBS and**
 87 **intraperitoneal delivery of anti-anti-PD-L1 antibody (E, F), after intratumoral injection of Heat-**
 88 **MVA and intraperitoneal delivery of isotype antibody control (G, H), after intratumoral injection**
 89 **of Heat-MVA and intraperitoneal delivery of anti-CTLA-4 antibody (I, J), after intratumoral**
 90 **injection of Heat-MVA and intraperitoneal delivery of anti-PD-L1 antibody (K, L). (M) Kaplan-**
 91 **Meier survival curve of tumor-bearing mice treated with PBS (n=6), anti-CTLA4 antibody**
 92 **(n=7), or anti-PD-L1 antibody (n=7; ****P* < 0.001, Mantel-Cox test). (N) Kaplan-Meier survival**
 93 **curve of tumor-bearing mice treated with PBS (n=6), Heat-MVA + isotype control (n=10), Heat-**
 94 **MVA + anti-CTLA4 antibody (n=10), or Heat-MVA + anti-PD-L1 antibody (n=10; **P* < 0.05;**
 95 *****P* < 0.01; *****P* < 0.0001; Mantel-Cox test). A representative experiment is shown, repeated**
 96 **once.**



97 Fig. S10. **Intratumoral injection of Heat-iMVA is more effective than poly (I:C) in treating**
 98 **large established tumors.** (A) Schematic diagram of a unilateral tumor implantation model with
 99 large established B16-OVA model. B16-OVA melanoma cells (5×10^5 cells) were implanted
 100 intradermally to the right flanks of C57B/6 mice. 8-9 days after tumor implantation, mice were
 101 intratumorally injected with Heat-iMVA, poly (I:C), or PBS mock control twice weekly. Tumor
 102 sizes were measured and the survival of mice was monitored. (B) Volumes of injected tumors
 103 over days after injections with PBS, Heat-iMVA, or poly (I:C). (C) Initial tumor volumes on the
 104 day of first injection. (D) Kaplan-Meier survival curve of tumor-bearing mice treated with PBS,
 105 Heat-MVA, or poly (I:C) intratumorally (n=10; **P < 0.01; ****P < 0.0001; Mantel-Cox test).



106 Fig. S11. **The combination of intratumoral injection of Heat-MVA with systemic delivery of**
 107 **immune checkpoint antibodies has synergistic effect in curing large established B16-F10**
 108 **melanomas.** (A) Schematic diagram of a unilateral tumor implantation model with large
 109 established B16-F10 melanoma model. B16-F10 melanoma cells (5×10^5 cells) were implanted
 110 intradermally to the right flanks of C57B/6 mice. 8-9 days after tumor implantation, mice were
 111 intratumorally injected with 2×10^7 pfu of Heat-MVA twice weekly in the presence or absence
 112 of intraperitoneal delivery of anti-CTLA-4, anti-PD-1, or anti-PD-L1 antibodies. Tumor sizes
 113 were measured and the survival of mice was monitored. (B) Volumes of injected tumors over
 114 days after injections with PBS, or with Heat-iMVA in the presence of isotype control, or anti-
 115 CTLA-4, or anti-PD-1, or anti-PD-L1. (C) Initial tumor volumes prior to first treatment (n= 10;
 116 $*P < 0.05$; *t* test). (D) Kaplan-Meier survival curve of tumor-bearing mice treated with PBS, or
 117 Heat-iMVA in the presence of isotype control, or anti-CTLA-4, or anti-PD-1, or anti-PD-L1
 118 antibodies (n=10; $*P < 0.05$, $**P < 0.01$, $****P < 0.0001$; Mantel-Cox test).

mIFNA4 forward	5'-CCTGTGTGATGCAGGAACC-3'
mIFNA4 reverse	5'-TCACCTCCCAGGCACAGA-3'
mIFNB forward	5'-TGGAGATGACGGAGAAGATG-3'
mIFNB reverse	5'-TTGGATGGCAAAGGCAGT-3'
mIL6 forward	5'-AGGCATAACGCACTAGGTTT-3'
mIL6 reverse	5'-AGCTGGAGTCACAGAAGGAG-3'
mCCL4 forward	5'-GCCCTCTCTCTCCTCTTGCT-3'
mCCL4 reverse	5'-CTGGTCTCATAGTAATCCATC-3'
mCCL5 forward	5'-GCCACGTCAAGGAGTATTTCTA-3'
mCCL5 reverse	5'-ACACACTTGGCGGTTTCCTTC-3'
mCXCL10 forward	5'-GTCAGGTTGCCTCTGTCTCA-3'
mCXCL10 reverse	5'-TCAGGGAAGAGTCTGGAAAG-3'
mGAPDH forward	5'-ATCAAGAAGGTGGTGAAGCA-3'
mGAPDH reverse	5'-AGACAACCTGGTCCTCAGTGT-3'
hIFNB forward	5'-GCACTGGCTGGAATGAGACT-3'
hIFNB reverse	5'-CCTTGGCCTTCAGGTAATG-3'
hTNF forward	5'-AATAGGCTGTTCCCATGTAGC-3'
hTNF reverse	5'-AGAGGCTCAGCAATGAGTGA-3'
hIL6 forward	5'-AATTCGGTACATCCTCGACGG-3'
hIL6 reverse	5'-TTGGAAGGTTTCAGGTTGTTTTCT-3'
hCCL4 forward	5'-AAAACCTCTTTGCCACCAATACC-3'
hCCL4 reverse	5'-GAGAGCAGAAGGCAGCTACTAG-3'
hCXCL9 forward	5'-AAACCCAGATTCAGCAGATG-3'
hCXCL9 reverse	5'-TCTTTTGACGAGAACGTTGAGA-3'
hCXCL10 forward	5'-ATTTGCTGCCTTATCTTTCTG-3'
hCXCL10 reverse	5'-TCTCACCTTCTTTTTTCATTGTAG-3'
hGAPDH forward	5'-ATCAAGAAGGTGGTGAAGCA-3'
hGAPDH reverse	5'-GTCGCTGTTGAAGTCAGAGGA-3'

119 Table S1. **Primer sequences for quantitative real-time PCR for the expression of type I IFN,**
120 **proinflammatory cytokine and chemokine genes.**